JACS
JOURNAL OF THE AMERICAN CHEMICAL SOCIETY
Communication
pubs.acs.org/JACS

Spin Frustration in an Organic Radical Ion Salt Based on a Kagome-Coupled Chain Structure

Lars Postulka,[†] Stephen M. Winter,[†] Adam G. Mihailov,[‡] Aaron Mailman,[‡] Abdeljalil Assoud,[‡] Craig M. Robertson,[§] Bernd Wolf,[†] Michael Lang,[†] and Richard T. Oakley*[,‡]

[†]Physikalisches Institut, Goethe-Universität, Frankfurt 60438, Germany
[‡]Department of Chemistry, University of Waterloo, Waterloo, Ontario N2L 3G1, Canada
[§]Department of Chemistry, University of Liverpool, Liverpool L69 7ZD, United Kingdom

Supporting Information

ABSTRACT: Electro-oxidation of the quinoidal bisdithiazole BT in dichloroethane in the presence of $[Bu_4N][GaBr_4]$ affords the 1:1 radical ion salt $[BT][GaBr_4]$, crystals of which belong to the trigonal space group *P*3. The packing pattern of the radical cations provides a rare example of an organic kagome basket structure, with $S = 1/2$ radical ion chains located at the triangular corners of a trihexagonal lattice. Magnetic measurements over a wide temperature range from 30 mK to 300 K suggest strongly frustrated AFM interactions on the scale of $J/k_b \sim 30$ K, but reveal no anomalies that would be associated with magnetic order. These observations are discussed in terms of the symmetry allowed magnetic interactions within and between the frustrated layers.

Spin frustration arises when the geometrical constraints of a crystal lattice inhibit the antiparallel alignment of electron spins on different sites into magnetically ordered arrays.[1] This situation is generally found in select examples of transition-metal-based minerals and materials, where high lattice symmetry can give rise to triangular (Chart 1A) or tetrahedral arrangements of magnetic centers that enhance the classical spin degeneracy and offer the possibility for nonordered spin-liquid states to appear once quantum effects are included. Particularly attractive are systems possessing $S = 1/2$ moments, for which quantum fluctuations are stronger than higher spin counterparts, potentially leading to exotic spin-liquid states. For this reason, inorganic minerals and synthetic materials exhibiting triangular (B) and kagome[2] (C) architectures, with $S = 1/2$ metals located at the lattice vertices, have been extensively studied. Prominent examples include strongly insulating kagome derivatives of Herbertsmithite[3] and organic charge transfer salts based on pseudotriangular lattices.[4]

Chart 1

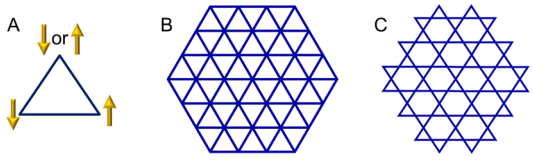

Hybrid metal−organic kagome-like structures displaying spin frustration have also been explored,[5] but examples of purely organic structures based on the kagome framework, and containing magnetically active $S = 1/2$ building blocks, are rare.[6] Here we report the preparation, structural and preliminary magnetic characterization of an organic radical salt that forms chain-like arrays locked into a distorted kagome packing pattern. The organic building block used here is the quinoidal bisdithiazole BT (Figure 1).[7] Antiaromatic, quasi-biradical[8] heterocycles of this type are easily oxidized to charge-transfer salts with a variety of stoichiometries,[9] and initial exploration of the redox chemistry of BT afforded $AlCl_4^-$ salts of both the radical cation $[BT]^+$ and closed-shell dication $[BT]^{2+}$.[7] A mixed valence salt $[BT]_2[GaCl_4]$ containing the dimer radical cation $[BT]_2^+$ was later described.[10]

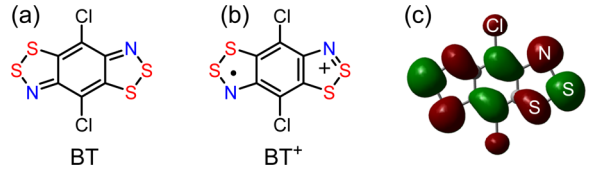

Figure 1. VB drawings of (a) BT, (b) its radical BT^+, and (c) the Kohn−Sham SOMO of the radical cation.

Crystals of the radical cation salt $[BT][AlCl_4]$ were tentatively assigned to the trigonal space group *P*3, but full structural elucidation was thwarted by twinning problems.[7] We have now found that blocks of the 1:1 tetrabromogallate salt $[BT][GaBr_4]$ suitable for single crystal X-ray diffraction can be generated by electro-oxidation of solutions of BT in the presence of $[Bu_4N][GaBr_4]$[11] in dichloroethane (DCE). The crystals belong to the trigonal space group *P*3 (Table S1) and consist of $[BT]^+$ radical cations packed into 2D arrays in the *ab* plane and displaying the trihexagonal tiling associated with the kagome basket (Figure 2). The $GaBr_4^-$ anions lie on 3-fold axes at (0, 0, *z*), (1/3, 1/3, *z*), and (2/3, 2/3, *z*), and the radical cations cluster about these axes with their mean molecular planes tilted to make an angle of 67.3° (at 100 K) with the *c*-axis. The *P*3 symmetry affords two distinct intermolecular S1···S4′ contacts d2 and d3 within the trihexagonal planes as well as

Received: May 17, 2016
Published: August 18, 2016

DOI: 10.1021/jacs.6b05079
J. Am. Chem. Soc. 2016, 138, 10738−10741

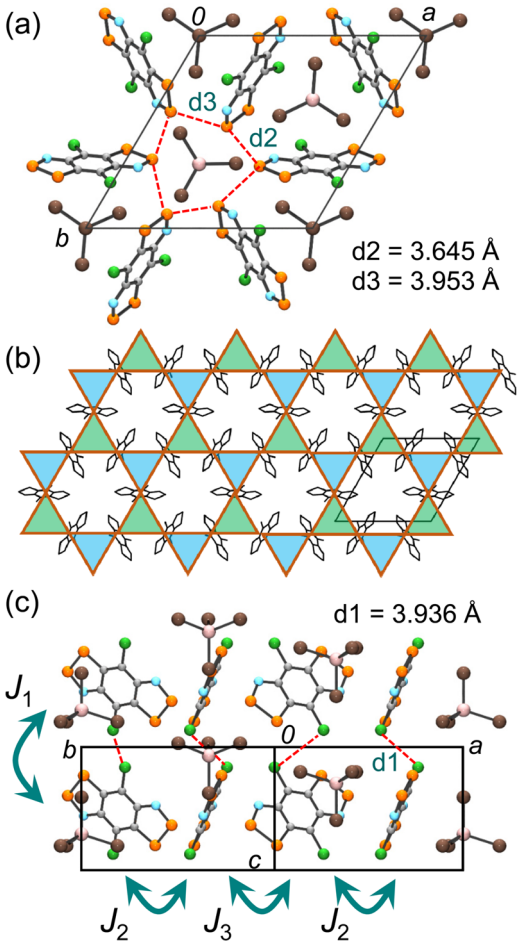

Figure 2. (a) Unit cell of [BT][$GaBr_4$], viewed parallel to the *c*-axis. (b) Trihexagonal tiling of the BT^+ radical cations in the *ab* plane. (c) Layers of BT^+ cations and $GaBr_4^-$ anions in the [110] plane, showing the three positions for the $GaBr_4^-$ ion. Intermolecular Cl1···Cl2′ (d1) and S1···S4′ (d2, d3) contacts (at 100 K) are shown with (red) dashed lines. Intermolecular exchange interactions J_1, J_2 (blue triangles) and J_3 (green triangles) are also defined.

a Cl1···Cl2′ interaction (d1) between adjacent layers along the *z*-direction; although outside the respective van der Waals separation,[12] these contacts are important in establishing magnetic communication (see below). At a molecular level, the internal structural metrics, notably the S−S distance, in the radical cation (Table S2) are slightly contracted relative to those in the parent heterocycle, as expected from the antibonding nature of the SOMO of the radical cation BT^+ (Figure 1). Pressed pellet conductivity measurements on [BT][$GaBr_4$] suggest Mott insulating behavior, with σ_{RT} near 10^{-6} S cm^{-1}, prompting investigation of its magnetic properties.

The crystallographic *P*3 symmetry allows three nearest-neighbor magnetic exchange interactions J_n (n = 1−3), which we define in magnitude and sign in terms of the Hamiltonian $H_{ex} = J_n \{S_i \cdot S_j\}$. As shown in Figure 2c, J_1 is associated with the long Cl1···Cl2′ contact (d1 = 3.936 Å) and links adjacent kagome layers, while J_2 (J_3) interactions occur within each layer in the blue (green) triangles shown in Figure 2b. The limit $J_1 \gg J_2$, J_3 describes decoupled 1D chains, while $J_1 \ll J_2$, J_3 gives decoupled kagome planes; within each such plane, the interactions are frustrated provided either J_2 or J_3 is antiferromagnetic (AFM). The results of variable-temperature field-cooled magnetic susceptibility (χ) measurements are shown in Figure 3.[13] Initial Curie−Weiss analysis of the χ versus T data provided a θ-value of +24.6 K, suggesting significant AFM coupling. A subsequent fit of this data over the range T = 2−300 K to a 1D AFM S = 1/2 chain model[14] (Figure 3b) indicated J_1 = +34.7 ± 0.5 K and zJ = +9 ± 4 K. The latter parameter zJ represents a mean-field interaction lateral to the 1D chains, and may be equated to $zJ \sim 2J_2 + 2J_3$. The slight deviation of this model from the experimental $\chi(T)$ for $T < zJ$ suggests the onset of interchain coupling effects beyond the mean-field approximation.

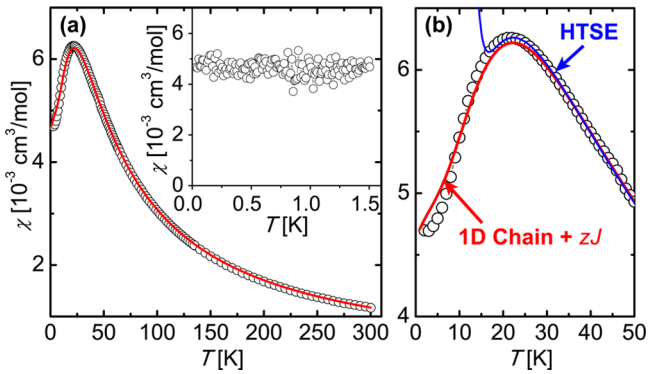

Figure 3. (a) Cooling curve plot from T = 2−300 K of χ versus T for [BT][$GaBr_4$] at H = 1 kOe, with a 1D AFM chain fit shown in red. Inset: Low-temperature susceptibility, showing absence of spin gap or ordered canted moment for T > 30 mK. (b) Zoom-in of $\chi(T)$ for T = 2−50 K, showing fitting results for 1D chain model (red) and HTSE approximation (blue) for J_1-J_2-J_3 model. As expected, the HTSE diverges below 20 K but provides an excellent fit for T = 20−300 K.

In order to further estimate the magnitude of these interchain interactions, we computed the high temperature series expansion (HTSE)[15] for χ up to eighth order in $(1/T)$ for the full J_1-J_2-J_3 model, which proved to be convergent for T = 20−300 K. Best fits for this model were obtained for J_1 = +30 K, J_2 = +16 K, and J_3 = −9 K, corresponding to zJ = +14 K. Taken together, these results suggest significant interactions both along the chains and within the layers. However, only a small separation between the experimental and fitted $\chi(T)$ profiles was observed down to 2 K. Due to the relatively low symmetry of the *P*3 space group, it is expected that magnetic order would produce a large increase in χ, as symmetry-allowed antisymmetric Dzyaloshinskii−Moriya interactions would promote a finite canted moment. To explore the possibility of ordering at lower temperatures, further $\chi(T)$ measurements were performed down to 30 mK (inset to Figure 3a). Below 2 K, the susceptibility was observed to saturate at a large value of about 4.7 × 10^{-3} cm^3 mol^{-1}, with no anomalies indicating ordering within the resolution of the experiment. The observation of finite χ at low temperatures $T \ll zJ$ also suggests a ground state with no energy cost for magnetic excitations, which argues against spin dimerization or short-ranged valence bond ground states. While these initial experiments do not allow for conclusive identification of the low-temperature magnetic state of [BT][$GaBr_4$], the results imply a possible gapless spin-liquid, such as the Luttinger state common in 1D antiferromagnets.[16]

Given these observations, it is insightful to consider three possible parameter regimes (i)−(iii) that can occur for trihexagonal [BT][X] materials consistent with a 1D-chain like response in $\chi(T)$, as shown in Figure 4. For the first case,

DOI: 10.1021/jacs.6b05079
J. Am. Chem. Soc. 2016, 138, 10738−10741

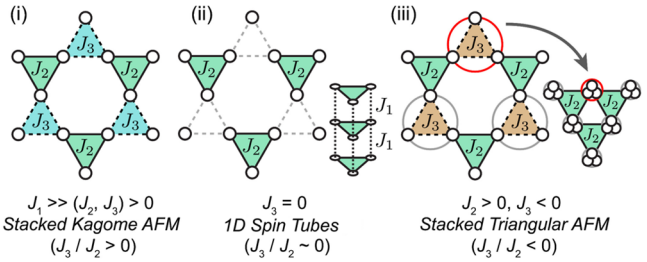

Figure 4. Possible magnetic models for [BT][$GaBr_4$] resulting from different values of J_1, J_2, and J_3. (i) Stacked kagome AFM, (ii) isolated three-legged spin tubes, and (iii) effective stacked triangular AFM lattice formed from local FM triangles.

(i) $J_1 \gg (J_2, J_3) > 0$ (stacked kagome AFM): If both J_2 and J_3 are AFM, then the kagome planes are fully frustrated, but for [BT][$GaBr_4$] the interactions must be dominated by the chain interaction J_1, in order to satisfy the condition that $J_1 \gg zJ$. It might be expected that the frustrated nature of the interchain interactions effectively decouples the chains,[17] resulting in a nearly 1D (spin-liquid) behavior. Quasi-1D behavior may also occur if one of the in-plane interactions is very small, leading to (ii) $J_3 = 0$, $J_2 = zJ/2$ (spin tubes). In this case, the spins are decoupled in the plane and form frustrated three-legged spin tubes running along the *c*-direction, with leg interactions J_1 and rung interactions J_2. A spin-gap is expected on the order of $\Delta \sim J_2/20-0.3$ K,[18] which is inconsistent with the low-temperature saturation of $\chi(T)$. We therefore consider this scenario unlikely for the present system and suggest that both interactions within the 2D layers must be significant. The final possibility (iii) $J_2 > 0$, $J_3 < 0$ (3D coupled FM triangles) is suggested by the HTSE fitting results. If one of the interactions within the trihexagonal plane is ferromagnetic, then the condition $J_1 \gg zJ$ may be satisfied even for significant intraplane interactions. In this case, a high spin $S = 3/2$ state would be favored on the FM triangles, resulting in an effective frustrated triangular lattice of FM coupled spins. The magnetic ground state would be expected to possess three sublattice magnetic order,[19] as in the $S = 3/2$ triangular lattice model, but fluctuations may suppress such order. In this way, a 1D chain-like response may appear over a broad temperature range despite significant J_2 and J_3, due to a combination of frustration decoupling of the chains and average cancellation of FM and AFM interactions. Future low-temperature-specific heat, ESR, NMR, and muon spin rotation experiments could further probe the magnetic ground state of [BT][$GaBr_4$], while nontrivial field-induced states might also be revealed in high-field magnetization measurements.[20]

At present, further insight into the magnetic state can be gained from density functional theory (DFT) estimates of the magnetic exchange interactions between pairs of radical cations. The pairwise exchange energies J_1, J_2, and J_3 (Figure 5) were calculated[21] at the UB3LYP/6-311G(d) level, using single point energies of the lowest triplet state E_{TS} and the broken symmetry singlet state E_{BSS} and their respective $\langle S^2 \rangle$ expectation values.[22] Given the strong interactions between the BT^+ cations and $GaBr_4^-$ anions, the latter were included in the calculations, in order to approximate the correct charge distribution on the organic component.[23] With their inclusion, the results are consistent with the HTSE fits, placing [BT][$GaBr_4$] in category (iii). The calculations afford a large AFM coupling $J_1 = +39$ K, while the lateral interactions J_2 and J_3 were found to be of similar magnitude but opposite sign, with $J_2 = +22.5$ K and $J_3 = -18.2$ K (and $zJ \sim 8$ K). The order of

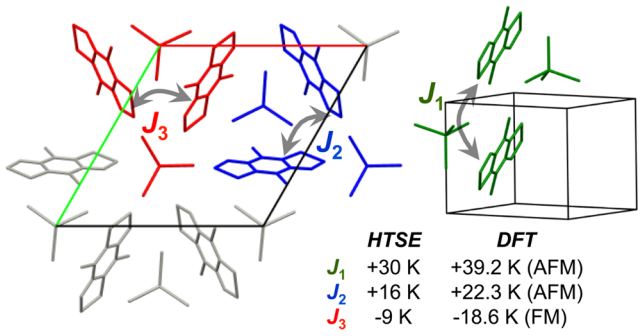

Figure 5. Magnetic exchange interactions J_1 (green), J_2 (blue), and J_3 (red) between pairs of radical cations in [BT][$GaBr_4$] and associated $GaBr_4^-$ anions (see text), with UB3LYP/6-311G(d) values calculated from crystal data at 100 K. The DFT values are compared to the results of HTSE fitting of $\chi(T)$.

magnitude of these interactions is consistent with that observed in related materials.[24] Inspection of the SOMO of the radical cation (Figure 1) suggests substantial spin density on the Cl centers, which mediates the J_1 interaction through Cl1···Cl2′ and Cl1···S2′ contacts despite the relatively far distance between adjacent kagome layers. The differing signs of the computed J_2 and J_3 may be related to the highly antibonding nature of the radical SOMO, which ensures a strong orientational dependence of the intermolecular orbital overlap, and related *J*-values.[25] This latter observation also suggests the possibility of tuning the dimensionality and frustration through chemical and physical pressure. A similar structure (space group *P*3) has already been demonstrated for [BT][$AlCl_4$],[7] and preliminary results indicate this packing motif can be generated for other tetrahedral anions. Furthermore, substitution of the exocyclic Cl atoms (by Br, I) may allow for adjustment of the interlayer coupling J_1.

In summary, geometrical spin frustration can be realized in [BT][X] materials as a result of the templating effect afforded by the three-fold symmetry of tetrahedral X^- anions. Accordingly the *P*3 crystal symmetry found for [BT][$GaBr_4$] generates arrays of triangular subunits in the lattice. The measured susceptibility of this material does not reveal any evidence for magnetic order or a spin gap down to 30 mK, which is 2 orders of magnitude smaller than the dominant magnetic interactions ($\theta = +25.3$ K). The influence of quantum fluctuations on the magnetic response can be further assessed in terms of the so-called frustration parameter $f = T_N(\mathrm{MF})/T_N(\mathrm{exp})$,[26] where the mean-field ordering temperature $T_N(\mathrm{MF})$ is given by θ in high-dimensional systems. On this basis, and assuming $T_N(\mathrm{exp}) < 30$ mK, $f > 100$ for [BT][$GaBr_4$]. However, if one takes into account the quasi-1D response of [BT][$GaBr_4$], it may be more appropriate to use the coupled chain expression $T_N(\mathrm{MF}) = 2\,S^2[J \cdot zJ]^{1/2} \sim 9$ K, in which case $T_N(\mathrm{MF})$ still exceeds the lowest measured temperature by a factor $f > 30$. Further studies are required to probe the magnetic ground state of this system, in order to confirm this picture. If magnetic order is to be found, it would likely be highly suppressed by quantum fluctuations and may be noncollinear (spiral or 120° order), as observed in other frustrated systems.[27] Finally, it remains to be seen how the combined effects of chemical and physical pressure will influence the magnetic interactions. It may be possible to explore materials in the [BT][X] family corresponding to all magnetic models shown in Figure 4i–iii through judicious crystal engineering.

DOI: 10.1021/jacs.6b05079
J. Am. Chem. Soc. 2016, 138, 10738–10741

■ ASSOCIATED CONTENT

Supporting Information

The Supporting Information is available free of charge on the ACS Publications website at DOI: 10.1021/jacs.6b05079.

Experimental details and data (PDF)

Crystal data for [BT][GaBr4] at 100 K (CIF)

Crystal data for [BT][GaBr4] at 296 K (CIF)

■ AUTHOR INFORMATION

Corresponding Author

*oakley@uwaterloo.ca

Notes

The authors declare no competing financial interest.

■ ACKNOWLEDGMENTS

We thank the Natural Sciences and Engineering Research Council of Canada for financial aid and a postdoctoral fellowship to S.M.W. and the Diamond Light Source for access to beamline I19. Work by L.P., B.W., and M.L. was supported by the Deutsche Forschungsgemeinschaft through the Trans-Regional Research Center SFB/TR 49.

■ REFERENCES

(1) (a) Ramirez, A. P. *Annu. Rev. Mater. Sci.* **1994**, *24*, 453. (b) Moessner, R.; Ramirez, A. P. *Phys. Today* **2006**, *59*, 24. (c) Greedan, J. E. *J. Mater. Chem.* **2001**, *11*, 37.

(2) Mekata, M. *Phys. Today* **2003**, *56*, 12.

(3) (a) Shores, M. P.; Nytko, E. A.; Bartlett, B. M.; Nocera, D. G. *J. Am. Chem. Soc.* **2005**, *127*, 13462. (b) Han, T.-H.; Helton, J. S.; Chu, S.; Nocera, D. G.; Rodrigues-Rivera, J. A.; Broholm, C.; Lee, Y. S. *Nature* **2012**, *492*, 406. (c) Pati, S. K.; Rao, C. N. R. *Chem. Commun.* **2008**, 4683.

(4) (a) Shimizu, Y.; Miyagawa, K.; Kanoda, K.; Maesato, M.; Saito, G. *Phys. Rev. Lett.* **2003**, *91*, 107001. (b) Yamashita, M.; Nakata, N.; Senshu, Y.; Nagata, M.; Yamamoto, H. M.; Kato, R.; Shibauchi, T.; Matsuda, Y. *Science* **2010**, *328*, 1246.

(5) (a) Moulton, B.; Lu, J.; Hajndl, R.; Hariharan, S.; Zaworotko, M. J. *Angew. Chem., Int. Ed.* **2002**, *41*, 2821. (b) Nytko, E. A.; Helton, J. S.; Müller, P.; Nocera, D. G. *J. Am. Chem. Soc.* **2008**, *130*, 2922. (c) Scriven, E. P.; Powell, B. J. *Phys. Rev. Lett.* **2012**, *109*, 097206.

(6) (a) Awaga, K.; Inabe, T.; Maruyama, Y.; Nakamura, T.; Matsumoto, M. *Chem. Phys. Lett.* **1992**, *195*, 21. (b) Awaga, K.; Okuno, T.; Yamaguchi, A.; Hasegawa, A.; Inabe, T.; Maruyama, Y.; Wada, N. *Phys. Rev. B: Condens. Matter Mater. Phys.* **1994**, *49*, 3975. (c) Matsushita, T.; Hamaguchi, N.; Shimizu, K.; Wada, N.; Fujita, W.; Awaga, K.; Yamaguchi, A.; Ishimoto, H. *J. Phys. Soc. Jpn.* **2010**, *79*, 093701.

(7) Barclay, T. M.; Cordes, A. W.; Goddard, J. D.; Mawhinney, R. C.; Oakley, R. T.; Preuss, K. E.; Reed, R. W. *J. Am. Chem. Soc.* **1997**, *119*, 12136.

(8) (a) Matsui, H.; Fukuda, H.; Hirosaki, Y.; Takamuku, S.; Champagne, B.; Nakano, M. *Chem. Phys. Lett.* **2013**, *585*, 112. (b) Takauji, K.; Suizu, R.; Awaga, K.; Kishida, H.; Nakamura, A. *J. Phys. Chem. C* **2014**, *118*, 4303.

(9) (a) Barclay, T. M.; Cordes, A. W.; Oakley, R. T.; Preuss, K. E.; Reed, R. W. *Chem. Mater.* **1999**, *11*, 164. (b) Barclay, T. M.; Burgess, I. J.; Cordes, A. W.; Oakley, R. T.; Reed, R. W. *Chem. Commun.* **1998**, *18*, 1939.

(10) Barclay, T. M.; Cordes, A. W.; Mingie, J. R.; Oakley, R. T.; Preuss, K. E. *CrystEngComm* **2000**, *2*, 89.

(11) Rudawska, K.; Ptasiewicz-Bąk, H. *J. Coord. Chem.* **2003**, *56*, 1567.

(12) (a) Bondi, A. *J. Phys. Chem.* **1964**, *68*, 441. (b) Dance, I. *New J. Chem.* **2003**, *27*, 22.

(13) Plots of ZFC-FC susceptibility vs T and field cycled M vs H measurements are provided in the Figures S4 and S5.

(14) Johnston, D. C.; Kremer, R. K.; Troyer, M.; Wang, X.; Klümper, A.; Bud'ko, S. L.; Panchula, A. F.; Canfield, P. C. *Phys. Rev. B: Condens. Matter Mater. Phys.* **2000**, *61*, 9558.

(15) Schmidt, H.-J.; Lohmann, A.; Richter, J. *Phys. Rev. B: Condens. Matter Mater. Phys.* **2011**, *84*, 104443.

(16) Giamarchi, T. *Quantum Physics in One Dimension*; Clarendon Press: Oxford, 2004.

(17) Schmalfuss, D.; Richter, J.; Ihle, D. *Phys. Rev. B: Condens. Matter Mater. Phys.* **2004**, *70*, 184412.

(18) Nishimoto, S.; Arikawa, M. *Phys. Rev. B: Condens. Matter Mater. Phys.* **2008**, *78*, 054421.

(19) Seki, K.; Okunishi, K. *Phys. Rev. B: Condens. Matter Mater. Phys.* **2015**, *91*, 224403.

(20) (a) Kawamura, H.; Miyashita, S. *J. Phys. Soc. Jpn.* **1985**, *54*, 4530. (b) Manaka, H.; Etoh, T.; Honda, Y.; Iwashita, N.; Ogata, K.; Terada, N.; Hisamatsu, T.; Ito, M.; Narumi, Y.; Kondo, A.; Kindo, K.; Miura, Y. *J. Phys. Soc. Jpn.* **2011**, *80*, 084714.

(21) Frisch, M. J.; Trucks, G. W.; Schlegel, H. B.; Scuseria, G. E.; Robb, M. A.; Cheeseman, J. R.; Scalmani, G.; Barone, V.; Mennucci, B.; Petersson, G. A.; Nakatsuji, H.; Caricato, M.; Li, X.; Hratchian, H. P.; Izmaylov, A. F.; Bloino, J.; Zheng, G.; Sonnenberg, J. L.; Hada, M.; Ehara, M.; Toyota, K.; Fukuda, R.; Hasegawa, J.; Ishida, M.; Nakajima, T.; Honda, Y.; Kitao, O.; Nakai, H.; Vreven, T.; Montgomery, J. A., Jr.; Peralta, J. E.; Ogliaro, F.; Bearpark, M.; Heyd, J. J.; Brothers, E.; Kudin, K. N.; Staroverov, V. N.; Kobayashi, R.; Normand, J.; Raghavachari, K.; Rendell, A.; Burant, J. C.; Iyengar, S. S.; Tomasi, J.; Cossi, M.; Rega, N.; Millam, N. J.; Klene, M.; Knox, J. E.; Cross, J. B.; Bakken, V.; Adamo, C.; Jaramillo, J.; Gomperts, R.; Stratmann, R. E.; Yazyev, O.; Austin, A. J.; Cammi, R.; Pomelli, C.; Ochterski, J. W.; Martin, R. W.; Morokuma, K.; Zakrzewski, V. G.; Voth, G. A.; Salvador, P.; Dannenberg, J. J.; Dapprich, S.; Daniels, A. D.; Farkas, O.; Foresman, J. B.; Ortiz, J. V.; Cioslowski, J.; Fox, D. J. *Gaussian 09*, Revision A.02; Gaussian, Inc.: Wallingford, CT, 2009.

(22) (a) Noodleman, L. *J. Chem. Phys.* **1981**, *74*, 5737. (b) Noodleman, L.; Davidson, E. R. *Chem. Phys.* **1986**, *109*, 131. (c) Nagao, H.; Nishino, M.; Shigeta, Y.; Soda, T.; Kitagawa, Y.; Onishi, T.; Yoshika, Y.; Yamaguchi, K. *Coord. Chem. Rev.* **2000**, *198*, 265. (d) Deumal, M.; Robb, M. A.; Novoa, J. J. *Prog. Theor. Chem. Phys.* **2007**, *16*, 271.

(23) Vela, S.; Jornet-Somoza, J.; Turnbull, M. M.; Feyerherm, R.; Novoa, J. J.; Deumal, M. *Inorg. Chem.* **2013**, *52*, 12923.

(24) (a) Deumal, M.; Rawson, J. M.; Goeta, A. E.; Howard, J. A. K.; Copley, R. C. B.; Robb, M. A.; Novoa, J. J. *Chem. - Eur. J.* **2010**, *16*, 2741. (b) Winter, S. M.; Cvrkalj, K.; Dube, P. A.; Robertson, C. M.; Probert, P. R.; Howard, J. A. K.; Oakley, R. T. *Chem. Commun.* **2009**, 7306.

(25) (a) Leitch, A. A.; Yu, X.; Winter, S. M.; Secco, R. A.; Dube, P. A.; Oakley, R. T. *J. Am. Chem. Soc.* **2009**, *131*, 7112. (b) Mito, M.; Komorida, Y.; Tsuruda, H.; Tse, J. S.; Desgreniers, S.; Ohishi, Y.; Leitch, A. A.; Cvrkalj, K.; Robertson, C. M.; Oakley, R. T. *J. Am. Chem. Soc.* **2009**, *131*, 16012. (c) Winter, S. M.; Hill, S.; Oakley, R. T. *J. Am. Chem. Soc.* **2015**, *137*, 3720.

(26) Balents, L. *Nature* **2010**, *464*, 199.

(27) (a) Yamada, A. *Phys. Rev. B: Condens. Matter Mater. Phys.* **2014**, *90*, 235138. (b) Ghorbani, E.; Tocchio, L. F.; Becca, F. *Phys. Rev. B: Condens. Matter Mater. Phys.* **2016**, *93*, 085111.

DOI: 10.1021/jacs.6b05079
J. Am. Chem. Soc. 2016, 138, 10738−10741